Earth Planets Space, **55**, 559–568, 2003

Mathematical simulation of magma-hydrothermal activity associated with the 1977 eruption of Usu volcano

Nobuo Matsushima

Geological Survey of Japan, AIST, 1-1-1 Higashi, Tsukuba, Ibaraki 305-8567, Japan

(Received September 3, 2002; Revised September 4, 2003; Accepted September 4, 2003)

During the 1977 eruption of Usu volcano, magma was emplaced at shallow crust. This intrusion induced fumarole activity immediately after the eruption. Based on the repeated thermal observations, the amount of heat discharged by this thermal activity is estimated to be 2×10^{17}J. The corresponding volume of the intrusion is 6×10^{7}m^3. The inferred intrusion volume is comparable to the volume of the resistive block beneath the major faults formed by this eruption, which was interpreted as a cooled intrusion on the basis of recently conducted MT surveys. The heat discharge rate is a surface boundary condition for an underlying magma hydrothermal system. A mathematical simulation, which accounts for multiphase mass and heat transport within a porous media, is conducted to reproduce the thermal activity of Usu volcano. The simulation incorporates the supply of latent heat by solidifying magma and heat transfer by degassing. Permeability conditions are important factors to fit the simulated heat discharge rate with the observation. Increased permeability of surrounding formations causes early appearance and high amplitude of surface heat discharge rate and reduced permeability causes opposite effect. The intrusion permeability has a strong influence on the surface thermal activity. High permeability is needed for the early appearance of the surface heat discharge rate, although it results in the maximum intrusion temperature that is much lower than the observed fumarolic temperature. To avoid the inconsistency, temperature dependent permeability is used in the simulation. The inside of the intrusion with the temperature dependent permeability that has low initial values and the high permeable margin are supposed to satisfy the conditions of the observed surface heat discharge rate and fumarolic temperature.

Key words: Magma-hydrothermal activity, heat discharge rate, Usu volcano.

1. Introduction

Thermal activities such as fumaroles and hot springs are observed at many volcanoes. Quantitative observations of these thermal phenomena provide some constraints on underlying magma-hydrothermal systems formed by the interaction between magma and groundwater within the volcano. Mathematical simulations of generic magma-hydrothermal systems for various heat source configurations and hydrological conditions, such as permeability and porosity, were conducted by Cathles (1977) and Norton and Knight (1977). Hayba and Ingebritsen (1997) simulated the multiphase groundwater flow near cooling plutons considering the temperature dependent rock permeability, and investigated the variation of flow pattern controlling the rock permeability, the presence of a caprock, size and emplacement depth of the pluton, the effect of multiple intrusions, and the influence of topography. They concluded that the host rock and pluton permeabilities are principal factor influencing fluid circulation and heat transfer in hydrothermal system.

During the 1977 eruption of Usu volcano, magma intruded the shallow crust (Okada *et al.*, 1981). The intrusion produced thermal activity just after the eruption (Yokoyama *et al.*, 1981). The heat discharge rates from 1975 to 1990 were investigated by repeated thermal observations (e.g. Kagiyama, 1984), and the volume of heat source was estimated (Matsushima, 1992). The 1977 intrusion was imaged by a recently conducted magnetotelluric study (Ogawa *et al.*, 1998; Matsushima *et al.*, 2002). Effective permeabilities and the hydrological structure of Usu volcano were estimated using wells drilled for hot spring exploitation at the foot of the volcano (Oshima and Matsushima, 1999). Application of these data (intrusion configuration, hydrological condition and surface boundary condition from heat discharge rate) to a mathematical simulation enables us to conduct a case study about the development of magma-hydrothermal system in an active volcano. In this paper, the heat discharge rate in 1999 is estimated and combined with the previous data to reveal the temporal variation of heat discharge rate over 20 years after the eruption. The volume of cooling intrusion is revaluated using the data. Next, results of a numerical simulation are presented in order to investigate the permeability conditions necessary for the development of thermal activity associated with the 1977 eruption of Usu volcano.

2. Shallow Intrusion of the 1977 Eruption

Usu volcano is a stratovolcano located in the southwestern part of Hokkaido, Japan (Fig. 1). In the 1.8-km diameter summit crater, a dacite lava dome formed in 1663 and 1853. At the foot of the volcano, many domes formed in 1910, and a lava dome, Showa-Shinzan, formed in 1943–1945 (Fig. 1).

In 1977, an eruption took place at the summit crater (Kat-

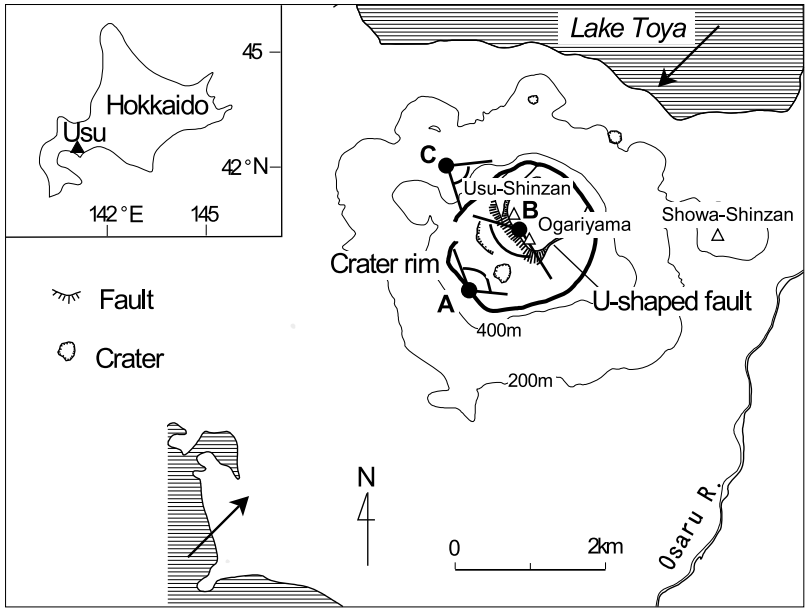

Fig. 1. Regional topographical map of Usu volcano and the observation sites for surface temperature in 1999 (solid circles). During the 1977–1978 eruption a steep slope was formed by the uplift of the northeastern side of a U-shaped fault. Two peaks at the edge of the slope are Usu-Shinzan and Ogariyama. Arrows indicate the resistivity cross section (Fig. 2).

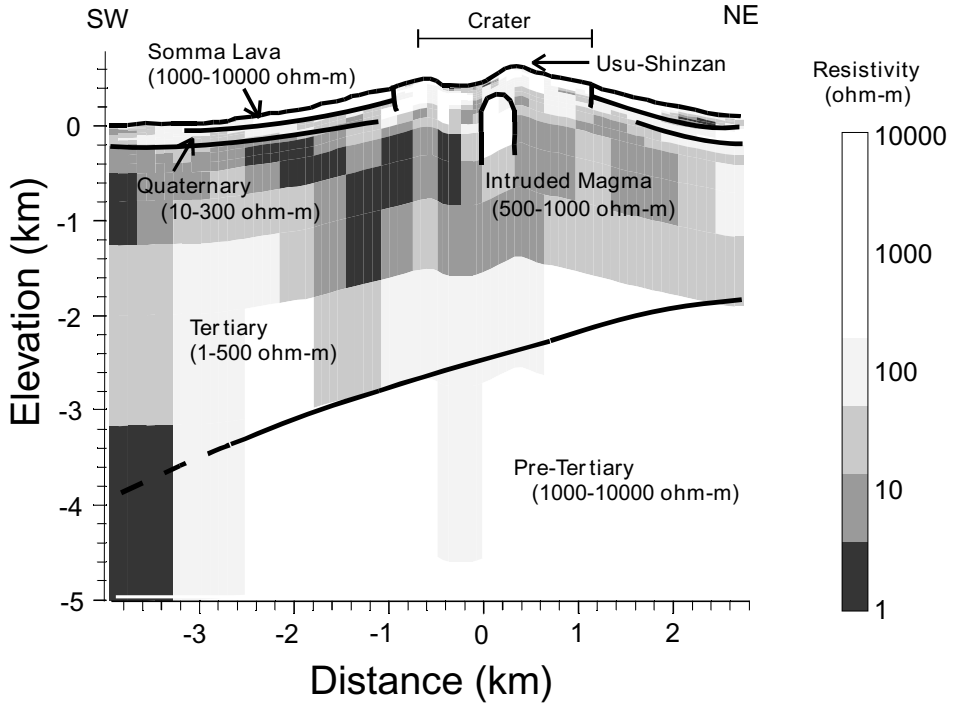

Fig. 2. Resistivity cross section obtained by the two-dimensional inversion of AMT and MT data and geological interpretation of the resistivity cross section.

sui *et al.*, 1978; Niida *et al.*, 1980; Yokoyama *et al.*, 1981). The first stage, from August 7 to 14, 1977, comprised major eruptions of dacite pumice; the second stage, from November 1977 to October 1978, comprised moderate phreatic, phreatomagmatic and magmatic eruptions. The second stage eruptions were concentrated in the southwestern part of the summit crater.

After the first stage eruptions, significant surficial movement formed a U-shaped fault in the summit crater (Fig. 1). On the northeastern side of the U-shaped fault, the ground was elevated by up to 180 m forming a steep slope along the fault. Two peaks at the edge of the slope are Usu-Shinzan and Ogariyama (Fig. 1). This conspicuous ground movement and frequent phreatomagmatic explosions implied the existence of a shallow magma intrusion. The daily uplift rate of Ogariyama-peak was observed from 1977 to 1979 (Yokoyama and Seino, 1979) and reached a maximum value (about 90 cm/day) in August 1977. After January 1978,

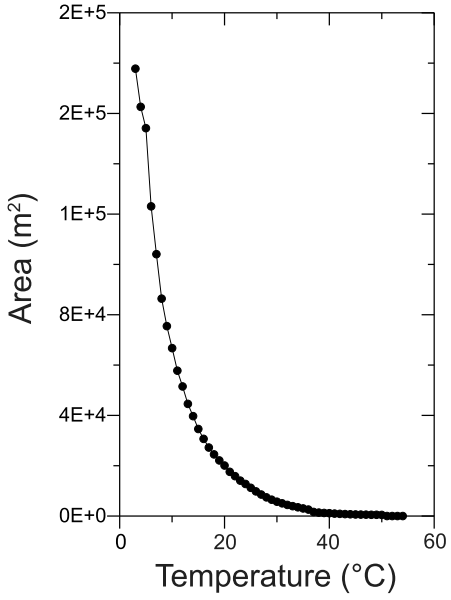

Fig. 3. Areas of temperature anomalies based on ground observation with an infrared thermal camera.

Table 1. Heat discharge observations for fumarole (Qp) and steaming ground (Qs).

Survey	Qp (MW)	Qs (MW)	Reference
09/75		1	Kagiyama (1978)
08/77		8	Matsushima (1992)
10/77		21	Matsushima (1992)
11/77	80		Kagiyama (1978)
02/78	310		Kagiyama (1978)
04/78		191	Matsushima (1992)
09/78		290	Matsushima (1992)
10/78	370		Kagiyama *et al.* (1984)
04/79	730		Sugoshi (1980)
09/79	420		Kagiyama *et al.* (1984)
11/79		320	Matsushima (1992)
12/79	360		Sugoshi (1980)
11/82	56		Kagiyama *et al.* (1984)
12/82	53		Kagiyama *et al.* (1984)
09/83	30	276	Tomiya (1983)
10/87		205	Matsushima (1992)
12/87	19		Matsushima (1992)
06/90	11		Matsushima (1992)
08/99		73	This study

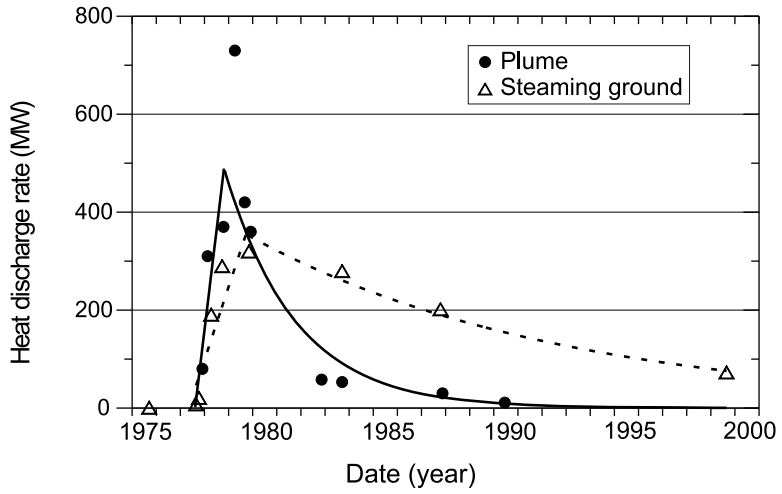

Fig. 4. Temporal variations of heat discharge rates from the active fumaroles (Qp, circles) and steaming ground (Qs, triangles).

the rate decreased exponentially to 10 cm/day in 1979. The uplift rate shows that the most magma intruded into the shallow crust until the early period of the second stage of the 1977 eruption.

Okada *et al.* (1981) analyzed volcanic earthquakes and detected an earthquake-free zone beneath the inside part of the U-shaped fault. Because earthquakes are caused by a failure of brittle rock, the presence of the earthquake-free zone suggests a magma intrusion. Moriya and Okada (1980) observed about a one second delay in travel times for earthquake waves passing through the earthquake-free zone. They concluded that a 1,000°C magma body caused this delay.

More recently, MT measurements revealed the underground structure of Usu volcano (Nishida *et al.*, 1996; Ogawa *et al.*, 1998). Figure 2 shows a two-dimensional resistivity section crossing Usu volcano from northeast to southwest (Matsushima *et al.*, 2002). A thick (2–4 km) conductive (1–500 Ω·m) layer of altered Tertiary volcanics is widely distributed. A resistive block (500–1,000 Ω·m) occurs in the Tertiary layer from 200 to 400 m beneath the summit crater, forming a striking contrast to the rest of the conductive Tertiary layer. A previous electrical survey (Watanabe *et al.*, 1984) did not observe this resistive block. Experimental measurements of rock resistivity (Murase, 1962) suggest that the resistivity of the intrusion increases dramatically with cooling. It was inferred that the resistive block represents the cooling intrusion associated with the 1977 eruption. The intrusion volume was $7 \times 10^7 m^3$, assuming the block had a cylindrical shape.

Airborne infrared surveys were conducted in 1975 (before the eruption), 1977, 1978, 1979 and 1983 (Yokoyama *et al.*, 1981; Geographical Survey Institute, 1980). The high temperature area was extended rapidly along the newly formed faults and craters just after the 1977 eruption. Most of the high temperature area is corresponded to steaming ground. There are many fumaroles in the central part of the steam-

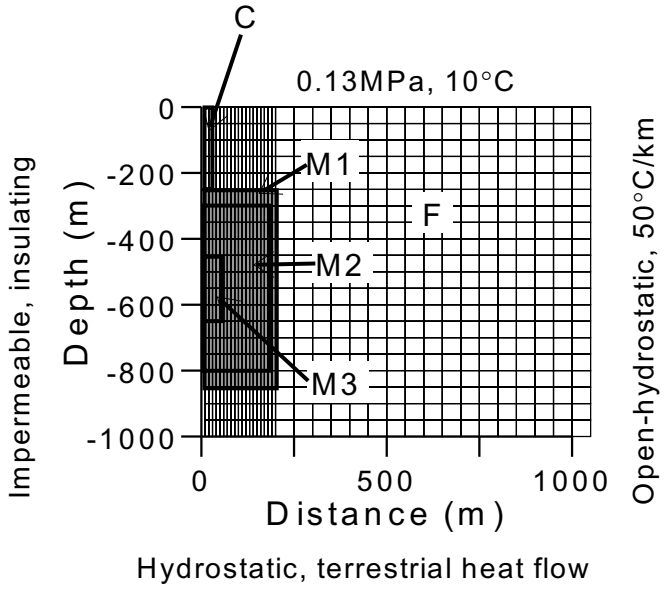

Fig. 5. Grid configuration and boundary conditions of the mathematical simulation.

Table 2. Permeability distribution of each model.

		F (m^2)	C (m^2)	$M1$(m^2)	$M2$ (m^2)	$M3$ (m^2)
model 1	K^H	10^{-11}	10^{-11}	10^{-12}	5×10^{-16}†	3×10^{-17}†
	K^V	10^{-12}	10^{-10}	10^{-12}	5×10^{-16}†	3×10^{-17}†
model 2	K^H	10^{-11}	10^{-11}	3×10^{-13}†	3×10^{-13}†	3×10^{-13}†
	K^V	10^{-12}	10^{-10}	3×10^{-13}†	3×10^{-13}†	3×10^{-13}†
model 3	K^H	10^{-11}	10^{-11}	10^{-12}	5×10^{-16}*	3×10^{-17}*
	K^V	10^{-12}	10^{-10}	10^{-12}	5×10^{-16}*	3×10^{-17}*
model 3′	K^H	10^{-11}	10^{-11}	10^{-12}	5×10^{-16}*	1×10^{-17}*†
	K^V	10^{-12}	10^{-10}	10^{-12}	5×10^{-16}*	1×10^{-17}*†
model 4	K^H	10^{-11}	10^{-11}	5×10^{-16}*†	5×10^{-16}*	3×10^{-17}*
	K^V	10^{-12}	10^{-10}	5×10^{-16}*†	5×10^{-16}*	3×10^{-17}*
model 5	K^H	10^{-11}	10^{-11}	10^{-12}	5×10^{-16}*	3×10^{-17}*
	K^V	3×10^{-12}†	10^{-10}	10^{-12}	5×10^{-16}*	3×10^{-17}*
model 6	K^H	10^{-11}	10^{-11}	10^{-12}	5×10^{-16}*	3×10^{-17}*
	K^V	10^{-13}	10^{-10}	10^{-12}	5×10^{-16}*	3×10^{-17}*

*Initial value of temperature-dependent permeability. The † indicates the difference from model 3.

ing ground. Some of these fumaroles have discharged superheated vapor since the eruption. The maximum fumarole temperatures were 700°C to 760°C in 1980–1985 and decreased gradually to 430°C in 1997 (Ossaka *et al.*, 1984; Japan Meteorological Agency).

3. Temporal Variation of Heat Discharge Rate

Thermal energy is mainly transmitted into the air by volcanic gas ejected from fumaroles (Qp) and steaming ground (Qs). The value of Qp can be obtained from photo images of the plume rising from fumaroles (Kagiyama, 1981). The Qs can be obtained from infrared-thermal image (Sekioka and Yuhara, 1974). The heat discharge rates from Usu volcano had been investigated by Kagiyama (1978), Kagiyama *et al.* (1984), Sugoshi (1980), Tomiya (1983) and Matsushima (1992) using above methods (Table 1).

In addition to these studies, the heat discharge rate from steaming ground in 1999 is investigated in this study. Surface temperature was measured by ground surveys using an infrared thermal camera (Agema, Thermovision 470). The observation sites are shown in Fig. 1 (closed circles, A, B and C). Two solid lines at each site indicate the area of the surface temperature measurements. The Qs is expressed as (Sekioka and Yuhara, 1974);

$$Qs = K \cdot \sum \Delta T \cdot S \tag{1}$$

where ΔT (°C) is surface temperature anomaly, S (m^2) is the area with the temperature anomaly and K (W/m^2°C) is a coefficient showing the effect of radiation, latent heat transfer and sensible heat transfer. The empirical mean value of 35 (Sekioka, 1983) was used for the coefficient K in this paper. The relationship between S and ΔT was obtained from the infrared-thermal image (Fig. 3). The heat discharge rate from the seaming ground is estimated to be 70 MW.

The compile of the previous data reveals the variation of heat discharge rates over 20 years after the 1977 eruption (Fig. 4). Both Qp and Qs rapidly increased immediately after the 1977 eruption and reached their respective maxima

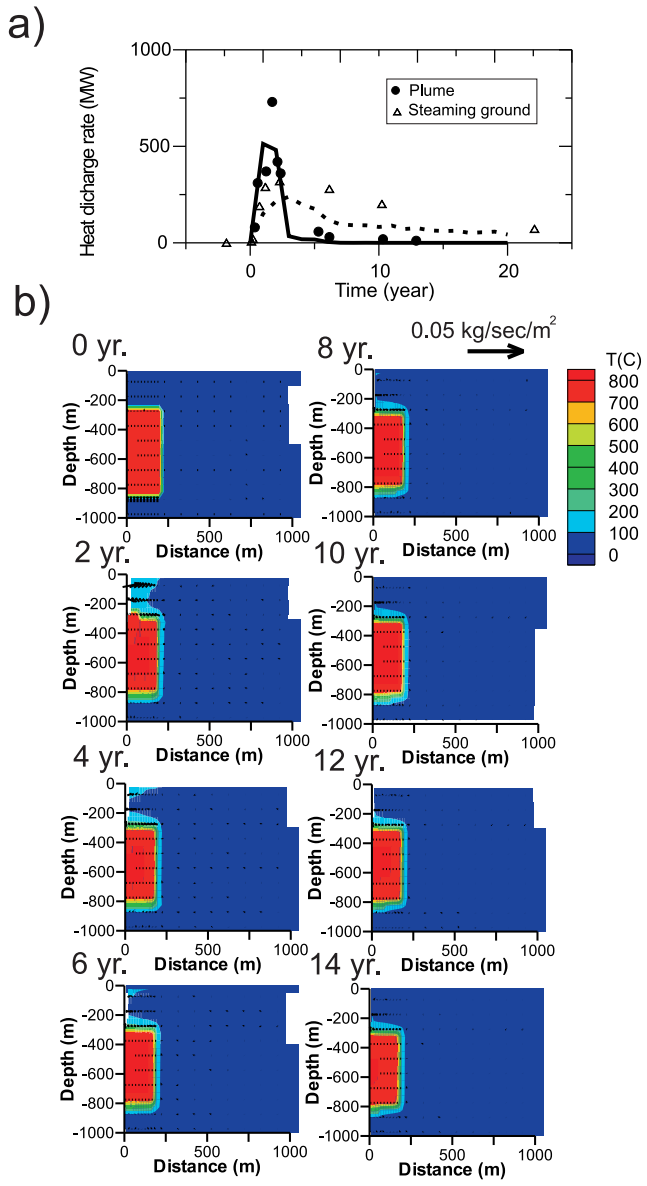

Fig. 6. Simulation results of model 1. (a) Temporal variation of heat discharge rate. Solid and dashed lines indicate the simulated heat discharge rate via vapor and hot water flow, respectively. Circles and triangles are the observed heat discharge rates from fumaroles and steaming ground, respectively. (b) Calculated temperature distributions (gray scale) and mass flow vectors (magnitude is proportional to the arrow length) at each year.

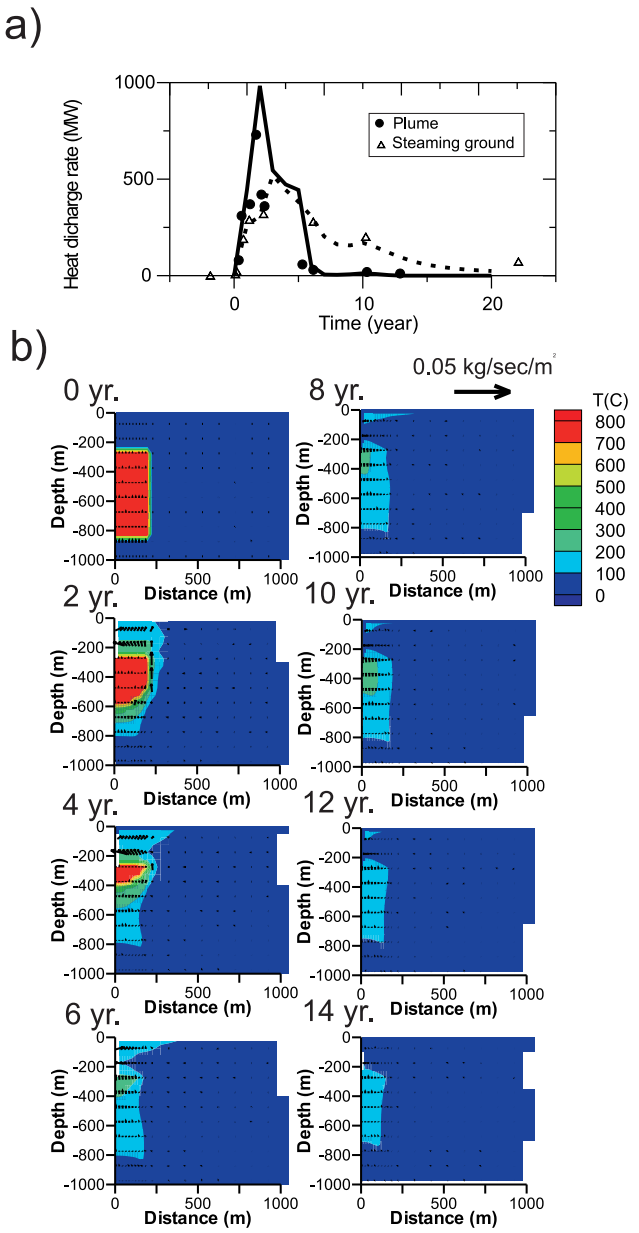

Fig. 7. Simulation results of model 2. (a) Temporal variation of heat discharge rate. (b) Calculated temperature distributions (gray scale) and mass flow vectors (magnitude is proportional to the arrow length) at each year.

of 700 MW and 300 MW in 1979. The decay of Qp was rapid (11 MW as of 1990), the decay of Qs relatively slow (70 MW in 1999). The Qp and Qs rates reached their maxima about two years after the magma intrusion. The subsequent rapid Qp decay is probably caused by a decrease in the quantity of superheated vapor rising through vents or faults. The slower Qs decay suggests a larger time constant for the hydrothermal convection under the crater floor, which was suggested by self-potential observations (Nishida and Tomiya, 1987; Matsushima *et al.*, 1990).

4. Volume of the Cooling Intrusion

From the heat released from the surface, we can estimate the volume of heat source (Matsushima, 1992). Following the previous work, the volume of the intrusion was revaluated using the newly compiled data. The total heat released from the cooling intrusion (Qt) is obtained as the integral of Qp and Qs over time. The Qp and Qs observations are fitted by straight lines from the onset of the eruption to the time of maximum Qp and Qs, thereafter with exponential curves. An infinite time integral is applied to the exponential curves. The calculated total heat is 2×10^{17}J. The corresponding volume of the intrusion is estimated to be $6 \times 10^7 \mathrm{m}^3$ assuming a heat capacity of 1300 J/kg·K (Birch *et al.*, 1954), latent heat of 4×10^5J/kg (Jeager, 1964), density of 2300 kg/m^3 and temperature decrease of 800°C. It is noticed that this volume is comparable to that of the cooled intrusion ($7 \times 10^7 \mathrm{m}^3$) inferred from MT surveys.

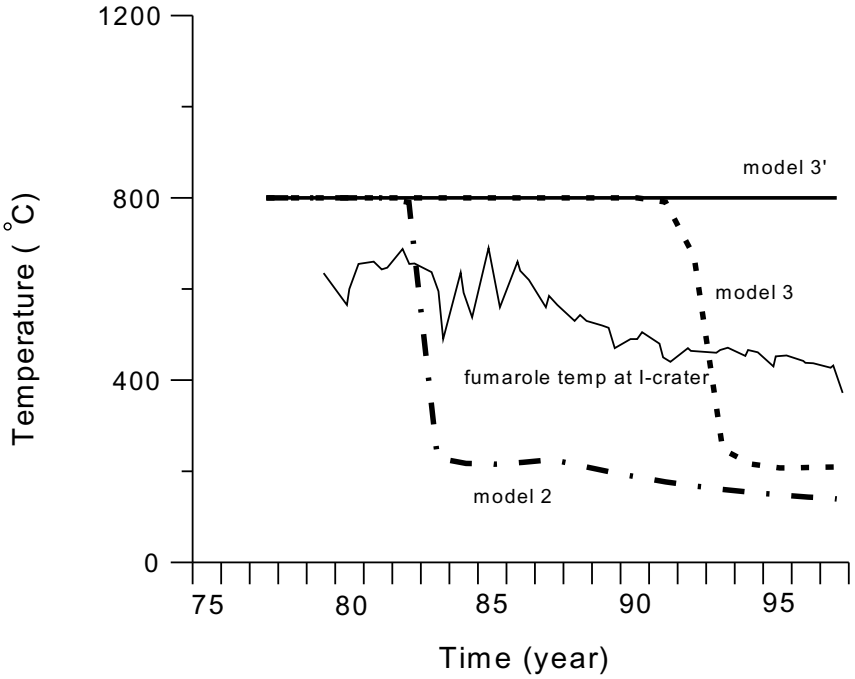

Fig. 8. Simulated maximum intrusion temperature for model 2, 3 and 3′ (thick lines), and observed fumarolic temperature at I-crater (thin line).

5. Mathematical Simulation of Magma-hydrothermal System of Usu Volcano

The simulator accounts for multiphase mass and heat transport within a porous media at temperatures from 0° to 800°C and pressures from 1 bar to 1 kbar (STAR; Pritchett, 1995). Darcy flow within a porous media is assumed. By solving conservation equations for mass and energy under initial and boundary conditions, pressure, temperature and phase condition are obtained. Physical properties of water such as viscosity and enthalpy are calculated from experimentally derived constituent equations.

5.1 Initial and boundary conditions

Grid geometry and boundary conditions are shown in Fig. 5. The simulation uses two-dimensional cylindrical coordinates. The boundary conditions for the upper surface, right side and lower surface are constant temperature and pressure. The right boundary is fixed because well logs at the foot of Usu volcano suggested that the high temperature area was limited to the summit area. Air temperature and pressure conditions are used for the upper surface boundary. Initial temperature and pressure are calculated from terrestrial heat flow and hydrostatic pressure gradient, respectively. An intrusion is assumed to be located in the area corresponding to the resistive block observed by MT surveys (600 m high and 200 m radius as shown in Fig. 5). The intrusion temperature is initially 800°C.

5.2 Rock properties of the formation

A porosity of 0.3 and thermal conductivity of 2.0 W/m°C are used in the entire region. Permeabilities are provided individually in five parts (F, C, $M1$, $M2$ and $M3$ in Fig. 5). Here, F corresponds to the Quaternary and Tertiary formations, and C corresponds to vent and faults filled with ash and volcanic rocks, respectively. $M1$, $M2$ and $M3$ correspond to the intrusion (shaded area in Fig. 5). Pumping tests on wells at the foot of the volcano suggest that the permeability of F and C would range from 10^{-10}m^2 to 10^{-15}m^2 (Oshima and Matsushima, 1999).

5.3 Latent heat and degassing

Heat of 6×10^{16}J is released from the solidifying intrusion, assuming a magma latent heat of 4×10^5J/kg, magma volume of 7×10^7m^3 and magma density of 2300 kg/m^3. The maximum fumarole temperature remained above 600°C until 1986, suggesting that parts of the intrusion were above the solidus temperature. Assuming the magma solidification during the twenty years after the 1977 eruption, the average increase of the heat discharge rate would be 100 MW during that period. Because we do not have detailed information of the solidification process, the effect of latent heat is simply incorporated into the heat source. If the intrusion temperature exceeds its upper limit (800°C), the accuracy of the calculation is reduced. To avoid the exceeding high temperature, it is assumed that the heat source depends on the initial and present temperatures of computation block. If the block temperature closes to the initial temperature, the heat source is ignored. The maximum potential heat source of 3 W/m^3 is prepared, with the restriction that the intrusion temperature does not exceed the initial temperature (800°C).

Total mass and heat of degassed water is estimated to be 5×10^9kg and 2×10^{16}J using a water content of 3 wt%, intrusion volume of 7×10^7m^3, intrusion density of 2300 kg/m^3 and water specific internal energy of 3.6×10^6J/kg. From the pressure dependence of water solubility and gas content within dacite magma, the degassing pressure was estimated to be 320 bars (New Energy and Industrial Technology Development Organization, 1993). At this pressure, 30% of the water content is degassed from the intrusion. The remaining water will be degassed with progressing solidification. An isotopic study showed that the highest magmatic gas content in the gas of the summit crater was observed in 1979 (Ossaka *et al.*, 1984). It is assumed that most of the water

content was degassed in the first two years after the eruption. The degassing is incorporated into the calculation as a mass source of the blocks just above the intrusion.

The estimated heat source with solidifying magma (6×10^{16}J) and degassing (2×10^{16}J) are one order magnitude smaller than the surface heat discharge (2×10^{17}J). For the Usu volcano thermal activity associated with 1977 eruption, heat released by the temperature decrease of the intrusion is an essential heat source.

6. Result

6.1 Basic cases—models 1 and 2—

The simulation results with constant intrusive permeability are presented for the basic case. When the permeability is small enough to prevent the convection inside the intrusion (model 1 in Table 2), the surface heat discharge rate is much smaller than the observation (Fig. 6(a)). In this case, the surface heat discharge is caused only by the degassing and vapor flow in the high permeable margin (Fig. 6(b)). The intrusion holds high temperatures for long period because the heat conduction is predominant inside the intrusion. When the intrusion has uniform permeability that is high enough to produce the vapor flow (model 2 in Table 2), the surface heat discharge is insistent with the observation (Fig. 7(a)). This model shows that the cooling of the intrusion progresses from below because heat loss is mainly due to upward movement of high temperature vapor and water (Fig. 7(b)). The maximum intrusion temperature of this model has cooled to 200°C at 5 years (Fig. 8). This temperature is much lower than the observed fumarolic temperature at I-crater (about 600°C as of 1982).

6.2 Time-dependent permeability—models 3 and 4—

Heterogeneous permeabilities are presumed to avoid the inconsistency between the calculated maximum temperature and observed fumarole temperature. As shown in Fig. 9(a), results using suitable permeability (model 3 in Table 2) approximate the observed heat discharge rate. The temperature dependent permeabilities are considered for the inside of the intrusion ($M2$ and $M3$), which have different low initial values. The variation of porosity by thermal stress is subjected to the formula prepared by the simulator (Pritchett, 1995) and Carman-Kozeny relation is used for the permeability calculation. The initial permeability values of $M2$ and $M3$ are assumed to have 5×10^{-16}m^2 and 3×10^{-17}m^2, respectively. The typical temperature dependence of permeability is presented in Fig. 10. The temperature dependent permeability introduces the vertical vapor flow at the intrusion margin (arrows in Fig. 9(b)). With the progress of the cooling, the flow area has shifted inside the intrusion. Considering the temperature dependent permeability for the intrusion make possible to maintain the high maximum intrusion temperature as shown in Fig. 8. Although, the maximum intrusion temperature in model 3 is also lower than the fumarolic temperature at 15 years. If we reduce the permeability of $M3$ by two factors, which hardly alter the surface heat discharge rate, the maximum temperature is still higher than the fumarolic temperature at 20 years (model 3′ in Table 2). In model 3, the intrusion margin ($M1$) is assumed to have constant high permeability (10^{-12}m^2). Without this high permeable zone (model 4 in Table 2), the simulated surface heat discharge

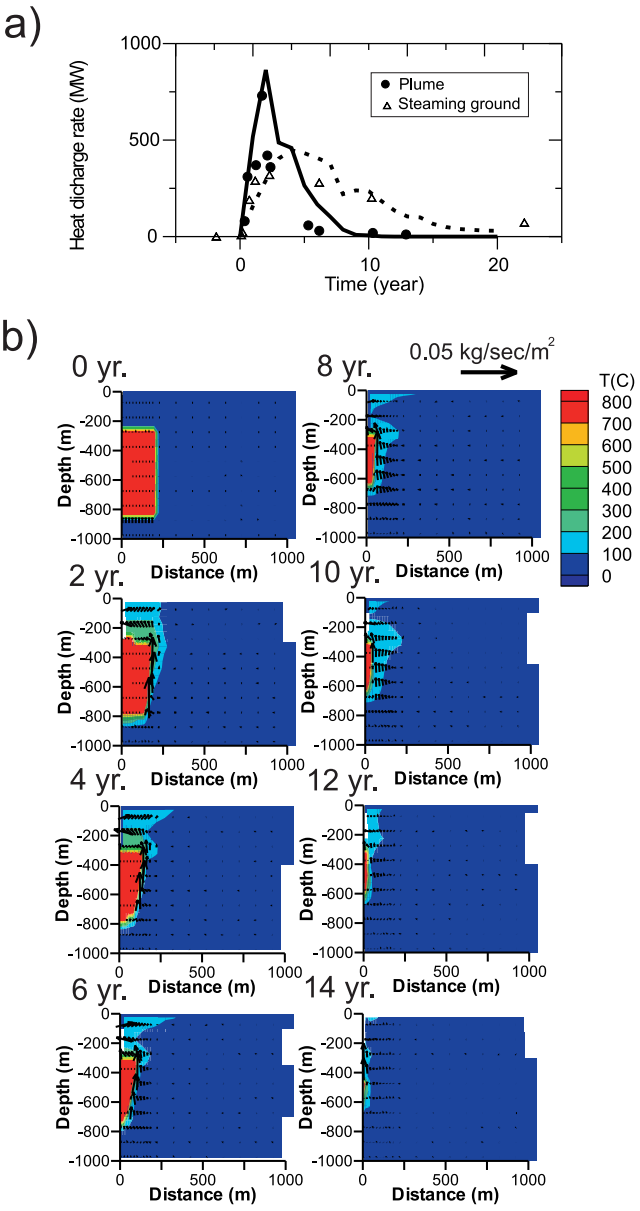

Fig. 9. Simulation results of model 3. (a) Temporal variation of heat discharge rate. (b) Calculated temperature distributions (gray scale) and mass flow vectors (magnitude is proportional to the arrow length) at each year.

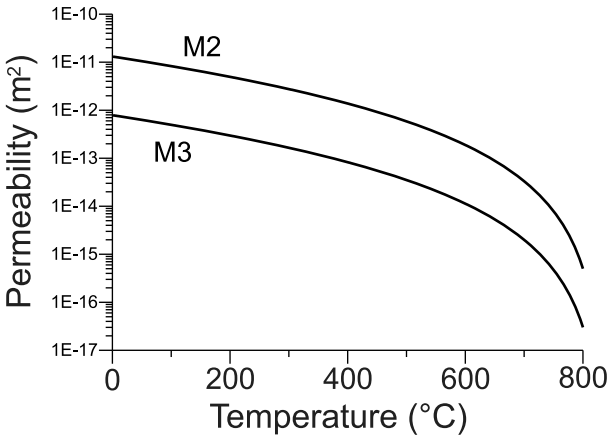

Fig. 10. Temperature dependence of intrusion permeability for $M2$ and $M3$ in Table 2.

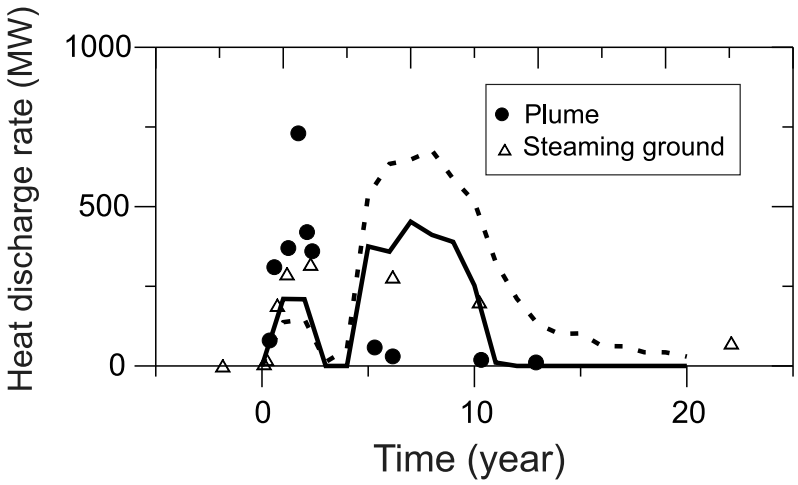

Fig. 11. Simulated heat discharge rate for model 4. Solid and dashed lines indicate the simulated heat discharge rate via vapor and hot water flow, respectively. Circles and triangles are the observed heat discharge rates from fumaroles and steaming ground, respectively.

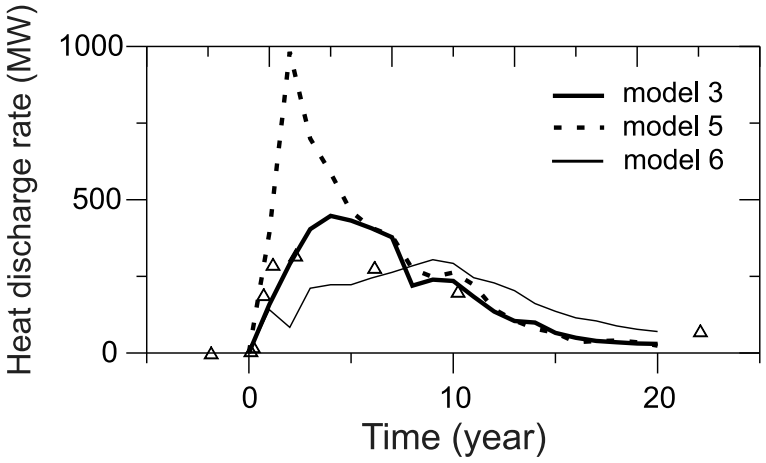

Fig. 12. Simulated temporal variations of heat discharge rate from steaming ground for model 3, 5 and 6.

rate is unlike with the observation (Fig. 11). This high permeable margin is needed to produce the rapid enhance of heat discharge rate at early period.

6.3 Influence of host rock permeability—models 5 and 6—

In the suitable model (model 3 in Table 2), host rock has following permeabilities: F of 10^{-11}m^2 (horizontal direction) and 10^{-12}m^2 (vertical direction), and C of 10^{-11}m^2 (horizontal direction) and 10^{-10}m^2 (vertical direction). The horizontal permeabilities of F and C are relatively insensitive to the reproduction of heat discharge rate. Appropriate horizontal permeabilities of F and C are from 10^{-12} to 10^{-11}m^2 that are higher than the general permeabilities of fractured rocks (e.g. Norton and Knapp, 1977). This result indicates that a sufficient water supply by a lateral flow is needed for the magma-hydrothermal system of Usu volcano. Lateral groundwater flow toward the intrusion accelerates the upward hot water and vapor flow within the intrusion. Although most of the vapor and hot water discharge into the air above the intrusion, the remaining vapor and hot water move outward near the surface. This lateral flow forms the high temperature steaming ground. The horizontal extent of the heated area is about 500 m, corresponding to the extent of the observed steaming ground. The result is consistent with the hypothesis that the heat discharge rate from steaming ground decayed slowly because it is linked to hydrothermal convection of thermal water.

The vertical permeability of host rocks (F) has a strong influence on the timing and magnitude of the peak heat discharge from steaming ground. Increased permeability value of F (model 5 in Table 2) leads to a faster and larger peak in the heat discharge rate from steaming ground (Fig. 12). Decreased permeability of F (model 6 in Table 2) has an opposite effect (Fig. 12). The area C corresponds to the vent and faults, which had developed with the remarkable crustal deformation (Katsui *et al.*, 1985). The formation of numerous faults just after the eruption had resulted in the rapid increase of heat discharge rate from fumarole (Qp). Although the vertical permeability of C had altered progressively with the development of the faults, it is assumed to be constant value of 10^{-10}m^2 in this simulation.

7. Discussion

In general, in situ measurements of fractured rock permeability indicate values in the range of 10^{-16} to 10^{-12}m^2 (Norton and Knapp, 1977). The permeability of 2.5×10^{-16}m^2

was assumed by Cathles (1977) in the simulation of cooling intrusives. In a two-phase hydrothermal cooling model for shallow intrusion, Carrigan (1986) assumed the cracking temperature of 725°C below which the intrusion is brittle enough to support crack formation caused by thermal stresses. The permeabilities from 10^{-12} to 10^{-14}m^2 were assumed at the cracking magma margins and impermeable magma was assumed at temperatures above the cracking temperature. The temperature-dependent permeability of intrusion was considered by Hayba and Ingebritsen (1997) in the simulation of multiphase groundwater flow near cooling plutons. They assumed that the intrusion permeability is negligibly low (10^{-22}m^2) at temperatures above 500°C and increases log linearly to 10^{-17}m^2 as temperature decreases from 500°C to 400°C. As temperature decreases further to 360°C (brittle/ductile transition), they assumed that the intrusion becomes as permeable as the surrounding host rock (permeabilities of 10^{-17}–$10^{-13.5}$m^2).

The presumed permeabilities of this paper are in the range of 10^{-17} to 10^{-10}m^2, which are higher than above values. For surrounding formation, the presence of high permeable fractured volcanic rocks (10^{-10} to 10^{-12}m^2) is suggested by in situ observation (Oshima and Matsushima, 1999). The high permeability in plastic magma (initial values of 10^{-16} and 10^{-17}m^2 inside magma and 10^{-12}m^2 at its margin) is possibly explained by the development of permeability in vesiculating magma (e.g. Blower, 2001). In this case, permeability is caused by the interconnection of bubbles, which is dissolved from magma. The magma with 3% water content results in 60% porosity (volume fraction of bubbles) at 700 m depths, if magma behaves as a chemically closed system during its ascent (Eichelberger *et al.*, 1986). The corresponding permeability becomes 10^{-14} to 10^{-12}m^2 (Eichelberger *et al.*, 1986; Klug and Cashman, 1996). The overall permeability has the values from 10^{-16} to 10^{-10}m^2 in the range of the porosity of 20 to 100% (Eichelberger *et al.*, 1986; Klug and Cashman, 1996). The shallow intrusion of Usu volcano probably included volatiles though it experienced major pumice eruptions at the initial stage (Watanabe, 1984). In addition to the thermal stress of cooling magma, the bubbles gradually formed by cooling or decompression inside magma probably play an important role to produce the high permeable magma hydrothermal system of Usu volcano.

This simulation suggests that the most of intrusion are sufficiently permeable at 20 years after the eruption. The connection of pore water will enhance the electrical conductivity, although the intrusion is detected as resistive block by MT measurement (Ogawa *et al.*, 1998). Another Quaternary intrusions also show high resistivity in Usu volcano (Nishida, 1988). Tertiary layer, which is widely distributed under the Usu volcano, is conductive because of the hydrothermal alteration (Matsushima *et al.*, 2002). In spite of the high permeable condition, the 1977 intrusion probably indicates relatively high resistivity, contrasting with the surrounding conductive Tertiary layer.

8. Summary

In the 1977 eruption of Usu volcano, magma intruded the shallow crust. The intrusion is a heat source for volcanic thermal activity that appeared immediately after the eruption. A total heat discharged by the thermal activity is estimated to be 2×10^{17}J. The corresponding intrusion volume is 6×10^7m^3. This volume agrees with the volume of the cooled intrusion observed by MT surveys.

A mathematical simulation is conducted to investigate the necessary conditions for development of the observed thermal activity. In the simulation, a heat and mass source are considered in the area corresponding to the resistive block. The permeability is important factor for the development of magma hydrothermal convection. When we consider suitable permeabilities for intrusion and host rocks, the simulation reproduce the observed heat discharge rate. The horizontal permeability of surroundings is higher than the values of representative fractured rocks, suggesting that lateral inflow is important for the development of hydrothermal convection. Lateral flow of vapor and hot water near the surface forms a high temperature area. The horizontal extent of the heated area is about 500 m corresponding to the observation. The host rock vertical permeability is sensitive to the elapsed time needed for the appearance of the maximum heat discharge rate from steaming ground. Increased permeability leads to a faster and larger peak in the heat discharge rate from steaming ground and decreased permeability has an opposite effect. The intrusion permeability has strong influence on the overall behavior of surface heat discharge. The relatively high intrusion permeability is needed for the rapid appearance of surface heat discharge. However, the high permeable condition also induces the rapid reduction of the intrusion temperature. In some case, the calculated temperature is inconsistent with the observed fumarolic temperature at I-crater. The inside of the intrusion with the temperature dependent permeability that has low initial values and the high permeable intrusion margin are presumed to satisfy the conditions of the observed surface heat discharge rate and fumarolic temperature.

Acknowledgments. I am grateful to the staff of the Usu volcano observatory of Hokkaido University for their assistance with the fieldwork. I thank Dr. Y. Nishida, Dr. H. Oshima and Dr. T. Ishido for their valuable comments and discussions. Critical and constructive reviews by Dr. S. Ingebritsen and Dr. T. Kagiyama have substantially improved the manuscript.

References

Birch, F., J. F. Schairer, and H. C. Spicer, *Handbook of Physical Constants,* Geological society of America special papers number 36, 1954.

Blower, J. D., Factors controlling permeability-porosity relationships in magma, *Bull. Volcanol.*, **63**, 497–504, 2001.

Carrigan, C. R., A two-phase hydrothermal cooling model for shallow intrusions, *J. Volcanol. Geotherm. Res.*, **28**, 175–192, 1986.

Cathles, L. M., An analysis of the cooling of intrusives by groundwater convection which includes boiling, *Econ. Geol.*, **72**, 804–826, 1977.

Eichelberger, J. C., C. R. Carrigan, H. R. Westrich, and R. H. Price, Non-explosive silicic volcanism, *Nature,* **323**, 598–602, 1986.

Geographical Survey Institute, Volcanic base map, Usu volcano, 1980.

Hayba, D. O. and S. E. Ingebritsen, Multiphase groundwater flow near cooling plutons, *J. Geophys. Res.*, **102**, 12235–12252, 1997.

Jeager J. C., Thermal effects of intrusions, *Reviews of Geophysics,* **2**, 443–466, 1964.

Kagiyama, T., Evaluation of heat discharge and H^2O emission from volcanoes—based on a plume rise assumption—, *Bulletin of the Volcanological Society of Japan*, **23**, 183–197, 1978 (in Japanese with English abstract).

Kagiyama, T., Evaluation methods of heat discharge and their applications to the major active volcanoes in Japan, *J. Volcanol. Geotherm. Res.*, **9**,

87–97, 1981.

Kagiyama, T., D. Shimozuru, H. Tomiya, T. Maekawa, and A. Suzuki, Thermal Survey of Usu volcano—Analysis of infrared imagery and successive photographs of fumarolic plume—, Joint Geophysical and Geochemical observations of Usu volcano in 1982 and Tarumai volcano in 1983, pp. 87–104, 1984 (in Japanese with English abstract).

Katsui, Y., Y. Oba, K. Onuma, T. Suzuki, Y. Kondo, T. Watanabe, K. Niida, K. Uda, S. Hagiwara, T. Nagao, J. Nishikawa, M. Yamamoto, Y. Ikeda, H. Katagawa, N. Tsuchiya, M. Shirahase, S. Nemoto, S. Yokoyama, T. Soya, T. Fujita, K. Inaba, and K. Koide, Preliminary report of the l977 eruptlon of Usu volcano, *J. Fac. Sci., Hokkaido Univ., Ser. IV,* **18**, 385–408, 1978.

Katsui, Y., H. Komuro, and T. Uda, Development of faults and growth of Usu-shinzan cryptodome in 1977–1982 at Usu volvano, north Japan, *J. Fac. Sci., Hokkaido Univ., Ser. IV,* **21**, 339–362, 1985.

Klug, C. and K. V. Cashman, Permeability development in vesiculating magmas: implications for fragmentation, *Bull. Volcanol.*, **58**, 87–100, 1996.

Matsushima, N., Temporal variation of heat discharge rate associated with the 1977 eruption of Usu vovcano, Ph. D. Thesis, Hokkaido Univ., Sapporo, 1992 (in Japanese).

Matsushima, N., M. Michiwaki, N. Okazaki, R. Ichikawa, A. Takagi, and Y. Nishida, Self potential studies in volcanic areas (2) Usu, Hokkaido Komagatake and Me akan, *J. Fac. Sci., Hokkaldo Univ., Ser. VII,* **8**, 465–477, 1990.

Matsushima, N., H. Oshima, Y. Ogawa, T. Shinichi, S. Hideyuki, M. Utsugi, and Y. Nishida, Magma prospecting in Usu volcano, Hokkaido, Japan, using magnetotelluric soundings, *J. Volcanol. Geotherm. Res.*, **109**, 263–277, 2002.

Moriya, I. and Hm. Okada, Observation of a quarry blast in and around Usu volcano: travel time and propagation anomaly caused by magma, *Bulletin of the Volcanological Society of Japan,* **25**, 63–74, 1980 (in Japanese with English abstract).

Murase, T., Viscosity and related properties of volcanic rocks at 800°C to 1400°C, *J. Fac. Sci., Hokkaido Univ., Ser. VII,* **1**, 487–584, 1962.

New Energy and Industrial Technology Development Organization, *Preliminary Study of the Magma to Hydrothermal Transition Resources,* 280 pp, 1993 (in Japanese).

Niida, K., Y. Katsui, T. Suzuki, and Y. Kondo, The l977 eruption of Usu volcano, *J. Fac. Sci., Hokkaido Unlv., Ser. IV,* **19**, 357–394, 1980.

Nishida, Y., Subsurface structure of Usu volcano as inferred from geomagnetic, audiofrequency magnetotelluric and self-potential studies, Kagoshima international conference on volcanoes, proceedings, 350–353, 1988.

Nishida, Y. and H. Tomiya, Self-potential studies in volcanic areas (l) Usu Volcano, *J. Fac. Sci., Hokkaldo Univ., Ser. VII,* **8**, 173–190, 1987.

Nishida, Y., M. Utsugi, H. Oshima, T. Kagiyama, T. Inoue, Y. Morita, S. Shigehara, and T. Maekawa, Resistivity structure of Usu volcano as revealed by the magnetotelluric measurements, *Geophysical Bulletin of Hokkaido University,* **59**, 151–162, 1996 (in Japanese with English abstract).

Norton, D. and J. Knapp, Transport phenomena in hydrothermal systems: the nature of porosity, *Amer. J. Sci.*, **277**, 913–936, 1977.

Norton, D. and J. Knight, Transport phenomena in hydrothermal systems: cooling plutons, *Amer. J. Sci.*, **277**, 937–981, 1977.

Ogawa, Y., N. Matsushima, H. Oshima, S. Takakura, M. Utsugi, K. Hirano, M. Igarashi, and T. Doi, A resistivity cross-section of Usu volcano, Hokkaido, Japan, by audiomagnetotelluric soundings, *Earth Planets Space,* **50**, 339–346, 1998.

Okada, Hm., H. Watanabe, H. Yamasita, and I. Yokoyama, Seismological significance of the 1977–1978 eruptions and the magma intrusion process of Usu volcano, Hokkaido, *J. Volcanol. Geotherm. Res.*, **9**, 311–334, 1981.

Oshima, H. and N. Matsushima, Preliminary report on hydrological environment in the shallow part of Usu volcano, *Geophys. Bull. of Hokkaido Univ.*, **62**, 79–97, 1999.

Ossaka, J., J. Hirabayashi, and T. Ozawa, Chemical compositions of volcanic gases collected after 1977 eruption of Usu volcano, Joint Geophysical and Geochemical observations of Usu volcano in 1982 and Tarumai volcano in 1983, pp. 117–126, 1984 (in Japanese with English abstract).

Pritchett, J. W., *STAR User's Manual,* 1995.

Sekioka, M., Proposal of a convenient version of the heat balance technique estimating heat flux on geothermal and volcanic fields by means of infrared remote sensing, Memoirs Defense Academy, 23, 95–103, 1983.

Sekioka, M. and K. Yuhara, Heat flux estimation in geothermal areas based on the heat balance of the ground surface, *J. Geophys. Res.*, **79**, 2053–2058, 1974.

Sugoshi, T., Thermal study of Usu volcanic activity from 1977 to 1980, Mass. Thesis, Hokkaido Univ., Sapporo, 1980 (in Japanese).

Tomiya, H., An study on the thermal anomaly of Usu volcano, Mass. Thesis, Hokkaido Univ., Sapporo, 1983 (in Japanese).

Watanabe, H., Gradual bubble growth in dacite magma as a possible cause of the 1977–1978 long-lived activity of Usu volcano, *J. Volcanol. Geotherm. Res.*, **20**, 133–144, 1984.

Watanabe, H., H. Yamashita, and T. Maekawa, Electrical study of the 1977–1982 activity of Usu volcano, *Geophysical Bull. of Hokkaido University,* 43, 31–40, 1984 (in Japanese with English abstract).

Yokoyama, I. and M. Seino, Prediction of development in the l977–78 activities of Usu volcano with consideration for energy discharge, *J. Fac. Scl., Hokkaldo Univ., Ser. Vll,* **6**, 87–200, 1979.

Yokoyama, I., H. Yamashita, H. Watanabe, and Hm. Okada, Geophysical characteristics of dacite volcanism—The 1977–1978 eruption of Usu volcano—, *J. Volcanol. Geotherm. Res.*, **9**, 335–358, 1981.

N. Matsushima (e-mail: matsushima-n@aist.go.jp)